Phase transition of Zn_2SnO_4 nanowires under high pressure

X. Shen,[1] J. Shen,[1] S. J. You,[1] L. X. Yang,[1] L. Y. Tang,[2] Y. C. Li,[2] J. Liu,[2] H. Yang,[3] K. Zhu,[1] Y. L. Liu,[1] W. Y. Zhou,[1] C. Q. Jin,[1] R. C. Yu,[1,a)] and S. S. Xie[1]

[1]*Beijing National Laboratory for Condensed Matter Physics, Institute of Physics, Chinese Academy of Sciences, P.O. Box 603, Beijing 100190, People's Republic of China*

[2]*Institute of High Energy Physics, Chinese Academy of Sciences, Beijing 100039, People's Republic of China*

[3]*State Key Laboratory of Gansu Advanced Non-ferrous Metal Materials, Lanzhou University of Technology, Lanzhou 730050, People's Republic of China*

(Received 7 September 2009; accepted 2 November 2009; published online 9 December 2009)

In situ high-pressure angle dispersive x-ray diffraction experiments using synchrotron radiation on inverse spinel structure Zn_2SnO_4 nanowires were carried out with a diamond anvil cell at room temperature. The crystal symmetry becomes lower at around 12.9 GPa and an intermediate phase with an orthorhombic structure occurs. At about 32.7 GPa, a phase transition occurs accompanying a high-pressure phase. *In situ* Raman scattering investigation was also performed to explore the phase transition. In the pressure range 15.5–32.8 GPa, the intermediate phase is also detected and a high-pressure phase is observed above 32.8 GPa. The high-pressure phase is considered to possess the ambient pressure structure of $CaFe_2O_4$. © *2009 American Institute of Physics*.
[doi:10.1063/1.3268460]

I. INTRODUCTION

Optically transparent and electrically conducting oxides have attracted many scientists due to their unique optical and electronic properties[1,2] and widespread and successful applications in recent years,[3,4] such as smart windows, thin-film photovoltaic, flat-panel displays, polymer-based electronics, and architectural windows. Among them, binary oxides, such as ZnO and SnO_2, have been focused on mostly.[5,6] Ternary oxides, in contrast, which may show better property, are still less investigated. Typically, as an important example of ternary transparent conducting oxides (TCOs), Zn_2SnO_4 (ZTO) is considered as a transparent high resistivity semiconductor whose basic property is still not completely known.[7] Being similar with $CuFe_2O_4$, ZTO has an inverse spinel structure[2] consisting of alternating tetrahedra of ZnO_4 and octahedra of ZnO_6 or SnO_6 in the lattice. The schematic crystal structure is presented in Fig. 1. The Zn atom is centered at a ZnO_4 tetrahedron with four nearest-neighbor O atoms, while the equal numbers of Zn and Sn atoms are at the center of octahedra with six nearest-neighbor O atoms. The O atoms are positioned in the same way in all octants with 5/2 Zn atoms and 3/2 Sn atoms as the nearest neighbors. For common inverse oxide spinels, especially ternary oxides, they almost have a general chemical formula AB_2O_4 and exist with a cubic spinel structure or an orthorhombic structure determined by the experimental conditions.[2] As we know, there are two kinds of combinations of valence-state cations in spinels: II-III spinels and IV-II spinels.[8] ZTO belongs to the latter one. Any spinel can be described by the formula $(A_{1-x}B_x)[A_xB_{2-x}]O_4$. For ZTO, x equals to 1, showing a completely inverse case. Besides, the degree of inversion (x) in the TCO spinels is proposed to affect their electrical and optical properties.[9] The effect on electrical property is because of cation self-doping, while that on optical property may be due to a change in interconduction-band energy gaps. The ternary semiconductor ZTO has high electron mobility, high electrical conductivity, and attractive optical properties; thus it is suitable for a wide range of applications in many advanced technologies. For example, ZTO particles have been applied in dye-sensitized solar cells[10] and negative electrode material in Li-ion battery. Compared with the traditional ZnO and SnO_2 cells, a ZTO cell is more stable and has better performance. In addition, the ZTO thin film is found to respond sensitively to the nitrogen oxides[11] among the examined complex oxides with spinel structure. At room temperature, the electrical resistance of the polycrystalline spinel ZTO films is strongly affected by humidity, and the response and recovery time are very short.[12] Up to now, most of the works on ZTO have primarily been limited to ZTO thin

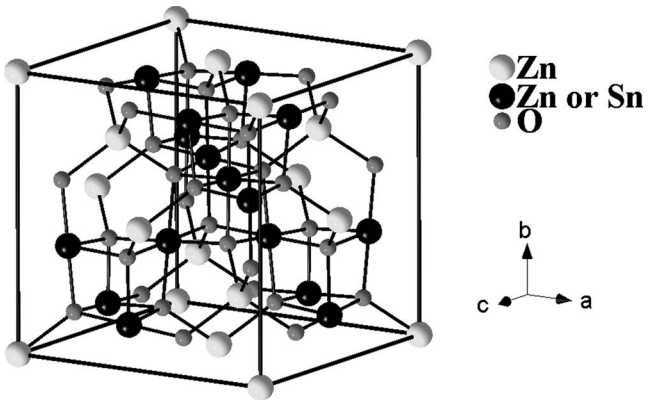

FIG. 1. The schematic model of the inverse spinel structure AB_2O_4 in one unit cell. The small balls represent the O atoms, the large light gray balls denote the Zn atoms occupying the center of the tetrahedral, and the large deep gray balls indicate an equal number of Sn and Zn atoms occupying randomly the center of the octahedra.

a)Author to whom correspondence should be addressed. Electronic mail: rcyu@aphy.iphy.ac.cn.

films.[9,11] Since the sizes and shapes of ZTO nanostructures[13] play very important roles in its electrical and optical properties,[14] it is very important to investigate structure characteristics of ZTO nanomaterials for revealing its significant property. Recently, high quality single crystalline ZTO nanowires were synthesized by a simple one-step thermal evaporation and condensation process.[15] As is well known, high pressure can modify the structural, electrical, and optical properties of materials,[16] so it is meaningful to study the structural stability of the inverse spinel structure ZTO under external pressure. In this paper, we report the structural behavior of ZTO nanowires under high pressure by angle dispersive x-ray diffraction (ADXD) and Raman spectrum measurements.

II. EXPERIMENTS

The details of synthesizing high quality single crystalline ZTO nanowires were described elsewhere.[15] *In situ* high-pressure ADXD experiments on ZTO were carried out with a diamond anvil cell (DAC) at room temperature, using synchrotron radiation at the Beijing Synchrotron Radiation Facility (BSRF).[17] The spot size and wavelength of the x-ray were 20×60 μm^2 and 0.6199 Å, respectively. The culet of the DAC was 300 μm in diameter. The sample powder was loaded with the ruby as pressure calibration into a 150 μm diameter hole in a T301 stainless steel gasket. Silicon oil was used as pressure medium. The ratio V/V_0 as a function of pressure P for the sample is obtained from the change in the spacing d between lattice planes obtained from the synchrotron x-ray diffraction experiments. Meanwhile, *in situ* Raman scattering investigation was conducted to explore the pressure-induced phase transformation of the inverse spinel-type ZTO at room temperature by a laser Raman spectrophotometer (HR800). The argon ion laser was tuned at 532 nm and the laser power was operated at 3 mW.

III. RESULTS AND DISCUSSION

In the ideal normal spinel crystal structure with a space group of $Fd3m$, there is a cubic close-packed array of anions with cations (A site atoms) occupying the center of tetrahedral in a face-centered-cubic (fcc) oxygen sublattice and B site atoms occupying the center of the octahedral. The crystal possesses a fcc structure and a unit cell has 32 anions and 24 cations. In the normal spinel structure, the cations occupy special positions 8a and 16d, while the anions occupy the general position 32e. In a typical inverse spinel structure, there exists competition between Sn atoms and Zn atoms at the center of octahedral (see Fig. 1). Ideally, to describe the inverse spinel structure, using a large supercell,[18] the centers of the octahedral are occupied randomly by Sn and Zn atoms.

In our experiments, the ZTO nanowires are with the size of about 150 nm in diameter. The purity of the synthesized ZTO nanowires was checked by XRD and all the sharp diffraction peaks can be indexed to a fcc inverse spinel structure with a space group of $Fd\bar{3}m$ and lattice parameter of $a=8.61\pm0.01$ Å, in consistent with the results in Ref. 2. And

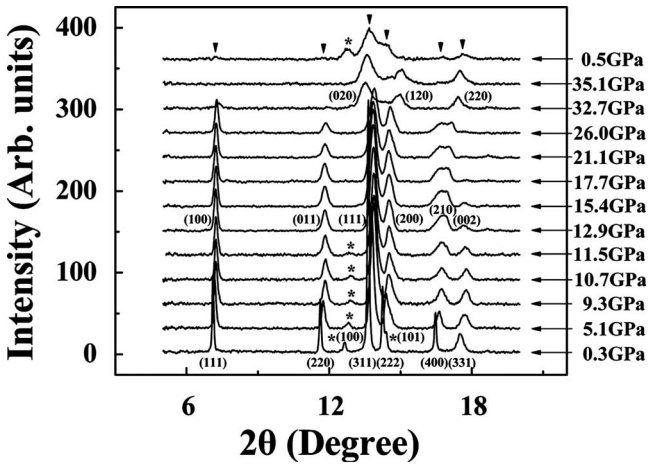

FIG. 2. ADXD patterns of the inverse spinel structure ZTO nanowires at different pressures.

the powder diffraction pattern matches very well with the standard data (see Ref. 19), showing the single phase of the sample.

Figure 2 presents the *in situ* ADXD patterns at different pressures up to 35.1 GPa. Six diffraction peaks (111), (220), (311), (222), (400), and (331) can be observed at ambient pressure. The peaks at $2\theta=12.8°$ and 14.3° plotted by " *" in Fig. 2 are (100) and (101) peaks of hexagonal ZnO (ZnO often occurs as less impurity when preparing ZTO), respectively; thus we do not take it into account in our analyses. When the pressure is raised to 10.7 GPa, no obvious changes occur in the diffraction patterns except for slight shifts of the peaks toward larger angle, showing the slight decrease in the lattice parameter. In the pressure range 12.9–26.0 GPa, the (400) peak happens to split and becomes two peaks with increasing pressure, and the (331) peak becomes weaker and disappears at around 17.7 GPa, indicating a distortion of crystal structure and appearance of an intermediate phase. By using DICVOL software, we tried to index the diffraction peaks of the intermediate phase that appeared at different pressures. The indexed results for the four data sets of the intermediate phase corresponding to the four pressures are consistent and the structure can be indexed to an orthorhombic structure with lattice parameters of $a=4.92$ Å, $b=4.36$ Å, and $c=4.19$ Å at 21.1 GPa. The diffraction peaks of the intermediate phase are indexed to be (100), (011), (111), (200), (210), and (002), respectively. At around 32.7 GPa, the peaks of the intermediate phase disappear completely and simultaneously three new peaks appear at $2\theta=13.5°$, 15.0°, and 17.4°, suggesting that a phase transition happens. The evolution of the diffraction peaks versus pressure is displayed in Fig. 3. According to the theory,[20] the higher is the ionicity of the defect chalcopyrite's material and the larger are the ionic-radius cations, the lower is the pressure needed for structural phase transition. So we can deduce that the ionicity of ZTO is lower than other inverse spinel phase $A^{IV}B_2^{II}O_4$ compounds (like Cd_2SnO_4) because of the higher pressure needed for the phase transition. After releasing pressure to 0.5 GPa, all the original peaks of the inverse spinel phase nearly come back to the original sites (as shown by ▼ at the top of Fig. 2), indicating the reversibility of the

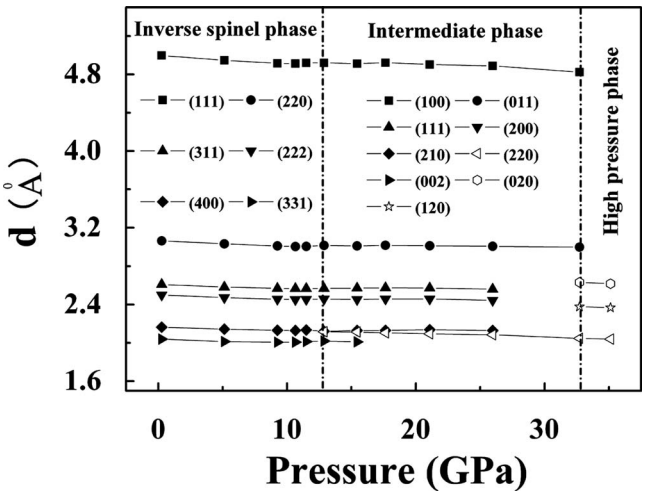

FIG. 3. The pressure dependence of d values of the sample peaks.

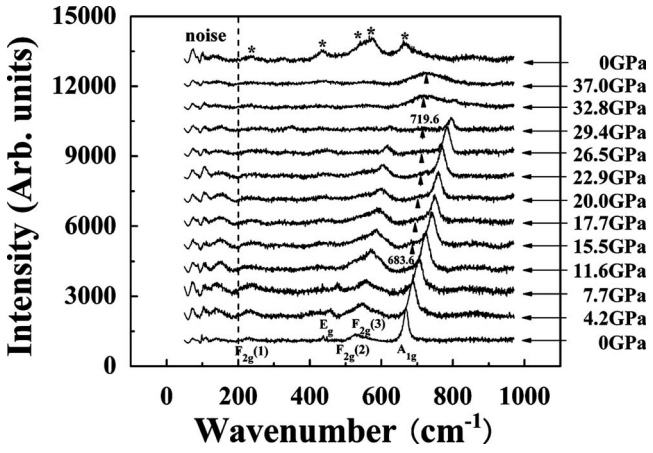

FIG. 4. Raman spectra of the inverse spinel structure ZTO at different pressures and room temperature.

phase transition in ZTO. The weakening of the intensities of the sample peaks at high pressure is due to the sample flowages out of the sample cell, and slight broadening of the peaks is caused by the sample thinning and pressure gradients in the sample under high pressure. The above results indicate clearly that for the inverse spinel structure ZTO nanowires, with increasing pressure, the intermediate phase occurs first at about 12.9 GPa and then a reversible crystal structural phase transition happens at about 32.7 GPa.

In general, the values of the unit cell volume as a function of pressure can be well derived from the refined lattice parameters. And the pressure-temperature-volume dependence can be decided systematically by an appropriate equation of state. The Birch–Murnaghan (BM) equation, being valid for the isotropic case, is described as

$$P = \frac{3}{2}\boldsymbol{B}_0\left[\left(\frac{V}{V_0}\right)^{-7/3} - \left(\frac{V}{V_0}\right)^{-5/3}\right]\left\{1 - \frac{3}{4}(4 - B_0')\right.$$
$$\left.\times\left[\left(\frac{V}{V_0}\right)^{-2/3} - 1\right]\right\}, \quad (1)$$

in which V and V_0 represent the volumes of the unit cell at pressure P and zero pressure, respectively, and B_0 and B_0' are the bulk modulus and its first-order pressure derivative. Through fitting the experimental data below 10.7 GPa by the BM equation, we obtain the bulk module B_0 =168.6(9.7) GPa, assuming its first-order derivative B_0'=4.

Figure 4 shows the Raman spectra of the ZTO nanowires at different pressures. In the spectrum at ambient pressure, the Raman mode near 226.5 cm^{-1} is quite weak, which may be caused by the overlapping effect with the laser-induced plasma,[21] and the two Raman peaks at 526.5 and 555.9 cm^{-1} indicate a highly inverse structure. For the highly inverse spinel structure ZTO, since the equal numbers of Zn and Sn atoms occupy the center of octahedral, the vibrations relating to Zn and Sn cations at the equal sites also induce two separated first-order Raman modes. As a result, the corresponding vibration peaks at 526.5 and 555.9 cm^{-1} with close vibrational frequencies result in an overlapped broad peak[22] (see Fig. 4). Besides this, the broadening of the Raman peaks is also a common feature of nanosize materials. From Fig. 4, we find that the main five sample peaks corresponding to different Raman active vibrational modes are similar to the situation of normal spinel structure $MgCr_2O_4$ at zero pressure. In order to study the vibrational modes further, we apply the nuclear site factor group analysis[23] and take into account the given positions of the atoms in the unit cell of inverse spinel structure ZTO, 8a position for Zn atoms, 16d position for an equal number of Zn and Sn atoms, and 32e position for oxygen atoms. Nikolic *et al.*[24] calculated and analyzed the following total number of active and inactive infrared reflection and Raman modes for the inverse spinel structure ZTO at ambient pressure:

$$\Gamma = 1A_{1g} + 1E_g + 3F_{2g} + 7F_{1u}, \quad (2)$$

where $1A_{1g}$, $1E_g$, and $3F_{2g}$ represent the five first-order active Raman modes while $7F_{1u}$ represents infrared modes and all these modes are observed in our experiments at ambient conditions, as shown in Table I and Fig. 5. The modes at 226.5, 438.6, 526.5, 555.9, and 668.3 cm^{-1} can be reasonably assigned to $F_{2g}(1)$, E_g, $F_{2g}(2)$, $F_{2g}(3)$, and A_{1g} symmetries, respectively.

Figure 4 presents the Raman spectra of the inverse spinel structure ZTO at different pressures and room temperature. Up to 11.6 GPa, all five modes of the inverse spinel structure shift mildly to the high wavenumber direction and the peak of E_g mode becomes undistinguishable at 11.6 GPa. In the pressure range 15.5–29.4 GPa, no distinguishable changes are observed either in the intensity or in the wavenumbers for the three modes: $F_{2g}(2)$, $F_{2g}(3)$, and A_{1g}. The Raman

TABLE I. The symmetry, the pressure dependence of Raman shifts, and the parameters of mode Gruneisen of the observed Raman modes of the inverse spinel structure ZTO at ambient conditions.

Raman mode (cm^{-1})	Assignment	Raman shift (cm^{-1}/GPa)	Mode Gruneisen parameter (γ_i)
226.5	$F_{2g}(1)$	1.33	0.99
438.6	E_g	4.99	1.92
526.5	$F_{2g}(2)$	3.26	1.04
555.9	$F_{2g}(3)$	1.84	0.56
668.3	A_{1g}	4.29	1.08

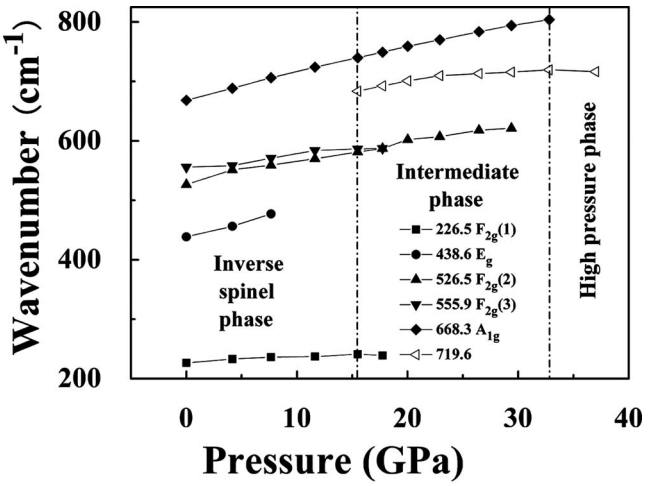

FIG. 5. The pressure dependence of the Raman modes of ZTO nanowires.

peak of $F_{2g}(1)$ mode disappears above 17.7 GPa, while a new peak at about 700.0 cm^{-1} grows continuously from 15.5 to 29.4 GPa, as shown in Fig. 4 (▲). The above results suggest that the intermediate phase exists in the pressure range 15.5–32.8 GPa, which is consistent with our *in situ* high-pressure ADXD measurements. Above 32.8 GPa, all the Raman modes corresponding to the intermediate phase completely disappear and only the new Raman peak of the high-pressure phase at 719.6 cm^{-1} shifts to high wavenumber direction with increasing pressure. Consistent with the high-pressure ADXD studies, the high-pressure Raman results also show that there is a phase transition in the inverse spinel structure ZTO nanowires beginning at about 15.5 GPa, causing the intermediate phase and transforming to a high-pressure phase at 32.8 GPa. The high-pressure structure of ZTO remains stable up to 37.0 GPa, the maximum pressure in our experiments. The pressure dependences of the observed Raman modes are plotted in Fig. 5 and concluded in Table I. The modes $F_{2g}(1)$, E_g, $F_{2g}(2)$, $F_{2g}(3)$, and A_{1g} of the inverse spinel structure ZTO display the pressure dependence of 1.33, 4.99, 3.26, 1.84, and 4.29 cm^{-1}/GPa, respectively, and the new mode of the high-pressure phase reveals a pressure dependence of 1.48 cm^{-1}/GPa. Therefore, we calculate the mode Gruneisen parameters (γ_i) according to the pressure dependences of the observed Raman modes for the inverse spinel and high-pressure structures (see Table I). Using the bulk modulus of ZTO calculated from the above ADXD data, the Gruneisen parameters (γ_i) at lower pressure range is obtained by the following equation:[22]

$$\gamma_i = -\left(\frac{d \ln \gamma_i}{d \ln P}\right) = \left(\frac{B_0}{\gamma_i}\right)\left(\frac{d\gamma_i}{dP}\right), \quad (3)$$

where γ_i indicates the Gruneisen parameter related to the ith vibration mode of the inverse spinel structure ($i=1-5$); P and B_0 represent pressure and bulk modulus at ambient conditions. Compared with the reported Raman spectra of normal spinel-type ferrite $ZnFe_2O_4$,[22] we find that they have similar Raman active vibrational modes and consistent evolution behavior under high pressure. According to group theory analyses (see Ref. 22), we can expect four types of Raman modes ($A_g, B_{1g}, B_{2g}, B_{3g}$) for the high-pressure phase of the normal spinel phase $ZnFe_2O_4$. Similar to $ZnFe_2O_4$, for the inverse spinel structure ZTO, five Raman modes, $F_{2g}(1)$, E_g, $F_{2g}(2)$, $F_{2g}(3)$, and A_{1g} change during phase transition. We consider that the E_g and A_{1g} modes transform to the A_g mode and the $F_{2g}(1)$, $F_{2g}(2)$, and $F_{2g}(3)$ modes transform to the $B_{1g}+B_{2g}+B_{3g}$ modes, referring to the rationale reported in Refs. 22 and 25. It was predicted that high-pressure phase $ZnFe_2O_4$ possesses ambient pressure structure of $CaFe_2O_4$.[22] Compared with the Raman modes of $CaFe_2O_4$ reported by Wang *et al.*,[26] we find Raman modes between the orthorhombic phase $CaFe_2O_4$ at zero pressure and the inverse spinel phase ZTO under high pressure are consistent. So it is reasonable to assume that the high-pressure phase of ZTO should have the zero-pressure structure of $CaFe_2O_4$. Therefore, in Fig. 2, the three sharp diffraction peaks that appeared at high pressures can be indexed to a primitive orthorhombic structure with a space group of *Pnam*. According to the indexed diffraction peaks (020), (120), and (220), the lattice parameters are calculated as $a=5.68$ Å and $b=5.26$ Å, while c cannot be determined yet due to few diffraction peaks in the ADXD patterns at high pressures. After releasing to ambient pressure, the five original Raman modes of the inverse spinel structure ZTO emerge again nearly at the original positions (as plotted by * in Fig. 4). Being consistent with the ADXD results, the Raman results also indicate that the phase transition is reversible. The broadening of the peaks of the pressure-released sample might be caused by the effect of the residual pressure in the sample.

IV. CONCLUSIONS

We utilized *in situ* high-pressure ADXD experiments and *in situ* high-pressure Raman scattering investigation to study the phase transition of ZTO nanowires under high pressure. With increasing pressure, an intermediate phase with an orthorhombic structure appears at 15.5 GPa and a high-pressure phase occurs at about 32.8 GPa. The high-pressure phase of ZTO is considered to possess the ambient pressure structure of $CaFe_2O_4$.

ACKNOWLEDGMENTS

This work was supported by the National Natural Science Foundation of China (Grant Nos. 10774168 and 50621061) and the State Key Development Project on Fundamental Research of China (Grant Nos. 2005CB623602 and 2010CB731600).

[1] L. S. Wang, X. Z. Zhang, X. Liao, and W. G. Yang, Nanotechnology **16**, 2928 (2005).
[2] D. Segev and S. Wei, Phys. Rev. B **71**, 125129 (2005).
[3] K. Nomura, H. Ohta, K. Ueda, M. Hirano, and H. Hoosono, Science **300**, 1269 (2003).
[4] S. Gao, Y. Zhao, P. P. Gou, N. Chen, and Y. Xie, Nanotechnology **14**, 538 (2003).
[5] M. H. Huang, S. Mao, H. Feick, H. Yan, Y. Wu, H. Kind, E. Weber, R. Russo, and P. Yang, Science **292**, 1897 (2001).
[6] Z. W. Pan, Z. R. Dai, and Z. L. Wang, Science **291**, 1947 (2001).
[7] S. M. Wang, Z. S. Yang, M. K. Lu, Y. Y. Zhou, G. J. Zhou, Z. F. Qiu, S. F. Wang, H. P. Zhang, and A. Y. Zhang, Mater. Lett. **61**, 3005 (2007).
[8] S. Wei and S. B. Zhang, Phys. Rev. B **63**, 045112 (2001).
[9] D. L. Young, D. L. Williamson, and T. J. Coutts, J. Appl. Phys. **91**, 1464 (2002).

[10]B. Tan, E. Toman, Y. G. Li, and Y. Y. Wu, J. Am. Chem. Soc. **129**, 4162 (2007).
[11]S. Matsushima, S. Kunitsugu, K. Kobayashi, and G. Okada, J. Ceram. Soc. Jpn. **103**, 302 (1995).
[12]I. Stambolova, K. Konstantinov, D. Kovavheva, P. Peshev, and T. Donchev, J. Solid State Chem. **128**, 305 (1997).
[13]J. X. Wang, S. S. Xie, H. J. Yuan, X. Q. Yan, D. F. Liu, Y. Gao, Z. P. Zhou, L. Song, L. F. Liu, X. W. Zhao, X. Y. Dou, W. Y. Zhou, and G. Wang, Solid State Commun. **131**, 435 (2004).
[14]R. R. He, M. Law, R. Fan, F. Kim, and P. D. Yang, Nano Lett. **2**, 1109 (2002).
[15]J. Shen, B. H. Ge, W. G. Chu, S. D. Luo, Z. X. Zhang, D. F. Liu, L. F. Liu, W. J. Ma, Y. Ren, Y. J. Xiang, C. Y. Wang, G. Wang, and W. Y. Zhou, Chin. Phys. B **17**, 2184 (2008).
[16]R. C. Yu, P. Zhao, F. Y. Li, Z. X. Liu, J. Liu, and C. Q. Jin, Phys. Rev. B **69**, 214405 (2004).
[17]J. Liu, J. Zhao, R. Z. Che, and Y. Yang, Chin. Sci. Bull. **45**, 1659 (2000).
[18]S.-D. Mo and W. Y. Ching, Phys. Rev. B **54**, 16555 (1996).
[19]JCPDS Card No. 74-2184.
[20]I. M. Tiginyanu, V. V. Ursaki, F. J. Manjon, and V. E. Tezlevan, J. Phys. Chem. Solids **64**, 1603 (2003).
[21]Z. W. Wang and S. K. Saxena, Solid State Commun. **118**, 75 (2001).
[22]Z. W. Wang, D. Schiferl, Y. S. Zhao, and H. S. C. O'Neill, J. Phys. Chem. Solids **64**, 2517 (2003).
[23]D. L. Rousseau, R. P. Bauman, and S. P. S. Porto, J. Raman Spectrosc. **10**, 253 (1981).
[24]M. V. Nikolic, T. Ivetic, D. L. Young, K. M. Parakevopoulous, T. T. Zorba, V. Blagojevic, P. M. Nikolic, D. Vasiljevic-Radovic, and M. M. Ristic, Mater. Sci. Eng., B **138**, 7 (2007).
[25]Z. Wang, H. S. C. O'Neill, P. Lazor, and S. K. Saxena, J. Phys. Chem. Solids **63**, 2057 (2002).
[26]Z. W. Wang, S. K. Saxena, and J. J. Neumeier, J. Solid State Chem. **170**, 382 (2003).